Submitted to Journal of Materials Research for Special Issue: Mechanical Properties and Microstructure of Advanced Metallic Alloys – in Honor of Prof. Hael Mughrabi

An examination of the superplastic characteristics of Al-Mg-Sc alloys after processing

Pedro H.R. Pereira [1], Yi Huang [1], Megumi Kawasaki [2,3], Terence G. Langdon [1,3*]

[1] Materials Research Group, Faculty of Engineering and the Environment, University of Southampton, Southampton SO17 1BJ, U.K.
[2] Division of Materials Science & Engineering, Hanyang University, Seoul 133-791, South Korea
[3] Departments of Aerospace & Mechanical Engineering and Materials Science, University of Southern California, Los Angeles, CA 90089-1453, U.S.A.

Abstract:

The Al-Mg-Sc alloys have become important materials in research conducted on superplasticity in aluminum-based alloys. Many results are now available and this provides an opportunity to examine the consistency of these data and also to make a direct comparison with the predicted rate of flow in conventional superplasticity. Accordingly, all available data were tabulated with divisions according to whether the samples were prepared without processing using severe plastic deformation (SPD) techniques or they were processed using the SPD procedures of equal-channel angular pressing or high-pressure torsion or they were obtained from friction stir processing. It is shown that all results are mutually consistent, the measured superplastic strain rates have no clear dependence on the precise chemical compositions of the alloys and there is general agreement, to within less than one order of magnitude of strain rate, with the theoretical prediction for superplastic flow in conventional materials.

Keywords: Al-Mg-Sc alloys; equal-channel angular pressing; friction stir processing; high-pressure torsion; superplasticity

*Corresponding author: Terence G. Langdon ; e-mail: langdon@soton.ac.uk ; Tel: +44-2380-593766.

PREAMBLE

We appreciate this opportunity to prepare a report honoring Professor Hael Mughrabi on the occasion of his 80th birthday. The senior author (TGL) has had many enjoyable and fruitful discussions with Hael over a period of about 40 years with numerous meetings in Europe and California. A highlight occurred in 1994 at the ICSMA Conference in Haifa when he had the pleasure of accompanying Hael and his wife Sybille on a visit to Hael's birthplace in Jerusalem. With this report, all of the authors send warmest greetings to Hael with our hopes and best wishes for many more productive years.

I. INTRODUCTION

When metals are pulled in tension, they generally break after pulling out to relatively low elongations. Nevertheless, under some limited experimental conditions it may be possible to achieve remarkably high neck-free elongations with samples pulling out to elongations up to and exceeding 1000%. This mode of flow is now called *superplasticity* and it was first demonstrated by Pearson in experiments conducted in the U.K. over 80 years ago when an elongation of 1950% was achieved in the tensile pulling of a Pb-Sn eutectic alloy [1]. Subsequently, there were many reports of superplastic flow in a range of metallic alloys and the ease of achieving high elongations led to the processing of these materials in metal forming applications and to the development of the important commercial superplastic forming industry. This industry is now used for the annual processing of thousands of tons of metals associated with the fabrication of complex shapes and curved parts for a wide range of uses in the aerospace and automotive sectors in addition to applications associated with architectural design and consumer products [2].

It is now recognized that two basic requirements must be fulfilled in order to achieve superplastic flow [3]. First, superplasticity occurs through the sliding of grains over each other within the polycrystalline matrix and this means the grain size must be very small and typically

less than ~10 μm. Second, since superplasticity is a diffusion-controlled process, it requires a relatively high testing temperature that is typically above ~0.5T_m where T_m is the absolute melting temperature of the metal. Generally, these two requirements are incompatible because the grains in a polycrystalline matrix grow easily at elevated temperatures and therefore it is not easy to retain very small grains for high temperature applications. Traditionally, most superplastic alloys have been prepared through the use of appropriate thermo-mechanical processing which reduces the grain size to within the range of ~3-10 μm. Generally, it has proven impossible using these procedures to reduce the grain size below 1 μm.

An alternative approach has become available over the last two decades which is based on an early report, appearing in 1988, describing both the ability to produce a submicrometer grain size through the application of severe plastic deformation (SPD) to a bulk coarse-grained Al-4% Cu-0.5% Zr alloy and also the potential for using this ultrafine-grained (UFG) material to achieve superplastic properties [4]. This early result and subsequent research has demonstrated that SPD processing provides opportunities for achieving grain sizes in the submicrometer or even the nanometer range and it is important to note that grains of these ultrafine dimensions cannot be attained using conventional techniques [5]. Several different methods of SPD processing have been developed [6] but attention has focused primarily on the two relatively simple procedures of equal-channel angular pressing (ECAP) and high-pressure torsion (HPT) [7]. In ECAP a sample, in the form of a bar or rod, is pressed through a die constrained within a channel which is bent through a sharp angle [8] whereas in HPT the sample, generally in the form of a thin disc, is subjected to a high applied pressure and concurrent torsional straining [9]. Both of these processes are effective in achieving exceptional grain refinement but HPT generally leads to smaller grains [10] and a higher fraction of high-angle grain boundaries [11].

Sufficient information is now available in the literature that it has become feasible to make a comprehensive review of the superplastic properties of a single selected material. The following section describes the background to producing superplastic elongations in aluminum and the later sections tabulate and analyze the data now available for Al-Mg-Sc alloys.

II. ACHIEVING SUPERPLASTICITY IN ALUMINUM

Aluminum is the most abundant metal in the Earth's crust and the most widely used non-ferrous metal. It has many applications including extensive use in the aerospace and transportation industries, in building construction and as a packaging material for a wide range of consumer products. Furthermore, early experiments showed that it was possible to process pure Al by ECAP to produce a grain size of ~1 μm which is within the range required for superplastic flow [12,13]. Nevertheless, superplasticity cannot be achieved in pure Al because the grains grow rapidly when the metal is heated to temperatures where diffusion occurs sufficiently rapidly. An alternative approach is to use an aluminum-based alloy such as the Al-3% Mg solid solution alloy which has also been studied extensively using SPD techniques [14,15]. This appears to be advantageous because the addition of Mg in solid solution in aluminum leads to smaller grain sizes such that the equilibrium grain size in an Al-3% Mg alloy is reduced to ~270 nm after processing by ECAP [16]. Nevertheless, superplasticity is again not easily achieved in an Al-3% Mg alloy because the UFG structure is stable only up to temperatures of ~500 K and at higher temperatures the grains grow very rapidly [17,18].

Early experiments showed that the advent of extensive grain growth may be delayed to ~600 K by adding Zr to the Al-Mg alloy [19,20] or to ~700 K through the addition of Sc [21]. Furthermore, very recent experiments on an Al-Mg-Sc-Zr alloy demonstrated excellent microstructural stability up to a temperature of ~800 K [22]. This suggests that Al-Mg-Sc alloys may be ideal candidate materials for achieving excellent superplastic properties after processing using SPD techniques.

An example of the superplastic properties of an Al-3% Mg-0.2% Sc alloy is shown in Fig. 1 where all tensile testing was conducted at 523 K using a constant rate of crosshead displacement with an initial strain rate of 1.0×10^{-3} s^{-1}: the upper specimen shows the initial shape of each sample and the four tensile specimens were prepared by ECAP through 8 passes (8p) at 300 K, ECAP through 10 passes at 600 K, HPT through 10 turns (10t) at 300 K and HPT through 10 turns at 450 K, respectively. It is readily apparent that all of these samples exhibit excellent superplastic properties.

Inspection of the literature shows that a large volume of data is now available describing the occurrence of superplasticity in various Al-Mg-Sc alloys. Accordingly, the following sections tabulate and provide a detailed analysis of these results.

III. SUPERPLASTICITY IN Al-Mg-Sc ALLOYS

In order to provide a meaningful tabulation of published data, it is first necessary to provide a precise definition of superplasticity. It was shown in very early work that the elongations achieved in tensile testing are directly proportional to the measured strain rate sensitivity, m [23,24]. Specifically, the ductility increases with increasing m and in superplastic flow the strain rate sensitivity is given by $m \approx 0.5$ which corresponds to a stress exponent of n $(= 1/m) \approx 2$. In solid solution alloys the flow process is often controlled by viscous glide where the moving dislocations drag atmospheres of solute atoms so that glide is the rate-controlling process. Under these conditions, the measured stress exponent is $n \approx 3$ so that $m \approx 0.3$ and there are often transitions in metallic solid solutions between the regimes of dislocation glide and dislocation climb [25,26]. It was noted in early research that high ductilities will be achieved also in solid solution alloys undergoing creep by viscous glide where $n \approx 3$ [27] and these high ductilities are now employed commercially in a hot blow-forming process to produce high volumes of panels of the AA5083 Al-Mg alloy for use in automotive applications

[28]. However, this behavior is outside of the regime of true superplasticity and it is better designated as "enhanced ductility" [29].

To avoid any overlap between results obtained in the viscous glide regime and in true superplastic flow, a critical review was undertaken of all available literature [30]. This review showed that elongations of up to and slightly exceeding 300% have been recorded during creep controlled by viscous glide [31] but there are no reports of any elongations at or above 400%. Accordingly, superplastic flow can be identified unambiguously as the achievement of tensile elongations of at least 400% and with an associated strain rate sensitivity of $m \approx 0.5$ [30].

Using this definition, a series of tabulations was prepared to record all results published to date showing true superplasticity in Al-Mg-Sc alloys. First, it is important to recognize that there are numerous reports of superplasticity in Al-Mg-Sc alloys even without processing using SPD procedures. These results are summarized in Table 1 [32-48] and they cover various metal-working procedures based primarily on cold- or hot-rolling. Typically, the grain sizes in these materials are in the conventional superplastic range of ~1 – 10 μm. For processing by SPD, results from ECAP are given in Table 2 where the grain sizes are now generally in the submicrometer range [49-79], Table 3 shows results for HPT where again the grain sizes are generally small [66,79-83] and Table 4 gives results for the alternative procedure of friction stir processing (FSP) [84-90] where FSP is a solid-state joining technique developed for Al alloys and with the capability of producing a UFG microstructure over a limited region of the sample [91,92]. In Table 2 many of the materials were processed at room temperature (RT), all ECAP dies had channel angles of 90° so that a strain of ~1 was introduced on each separate pass [93] and the various processing routes are defined as route A in which there is no rotation of the sample between passes, route B_C in which the rod is rotated by 90° around the longitudinal axis in the same sense between each pass and route C in which the rod is rotated by 180°, with route B_{CZ} relating to plate samples in which the plates are rotated in the same

direction by 90° around the vertical axis between each pass [94]. All of the ECAP samples exhibit excellent superplasticity with elongations up to and exceeding 2000%. Table 3 shows the applied pressure used in HPT and the dimensions of the samples where this is a critical parameter because of the use of small disks and the inherent limitations on the sample size. Nevertheless, HPT processing produces good superplastic elongations up to >1000%. Finally, in Table 4 the processing by FSP lists the geometry of the FSP tool, the rotation rate of the tool, the traverse speed for the processing, and again there are again excellent superplastic elongations. There is also a single recent report of elongations up to 1950% in an Al-3% Mg-0.2% Sc alloy processed by the new technique of high-pressure sliding (HPS) which is based on the principles of HPT and relates to two sheets sliding over each other during the processing operation [95].

IV. A COMPARISON OF DIFFERENT PROCESSING TECHNIQUES

The data summarized in Tables 1-4 represent four different processing procedures. In order to compare these different fabrication methods, it is appropriate to plot, for each separate processing technique, the results corresponding to the four highest reported elongations. These plots are shown in Figs 2 and 3 as the elongation versus temperature and the elongation versus the initial strain rate, respectively.

It is readily apparent from Fig. 2 that the elongations tend to increase with increasing temperature. Furthermore, excellent and similar results may be achieved using either ECAP or cold-rolling. Lower superplastic elongations are achieved when processing by HPT but this is attributed to the small size of the HPT specimens. Thus, although the measured elongations in tensile testing tend to increase with decreasing gauge length [96,97], the HPT specimens are cut from thin disks and their exceptionally reduced thicknesses of typically ~0.6 mm lead to easy and premature failure. This is evident from inspection of Table 3 where the maximum elongation of 1600% was achieved using a thicker specimen cut from a small cylindrical

sample [81]. The range of elongations achieved after FSP processing is due to the inhomogeneities that are an inherent feature of the localized and varying microstructural modifications that occur when using this type of processing.

Although the datum points in Fig. 3 are scattered, there is a general tendency to achieve higher elongations at faster strain rates. This is consistent with the very early demonstration that the exceptionally small grain sizes after SPD processing provide an opportunity for attaining superplasticity at high strain rates [98] where this is defined specifically as strain rates at and above 10^{-2} s^{-1} [99].

V. THE RATE-CONTROLLING FLOW PROCESS IN THE SUPERPLASTICITY OF Al-Mg-Sc ALLOYS

It is now well established that superplasticity occurs through the relative motion of adjacent grains in grain boundary sliding (GBS) [100]. However, the occurrence of superplasticity in isolation in a polycrystalline matrix will open cavities leading to premature failure. Instead there is now very good experimental evidence showing that the GBS in superplasticity is accommodated by dislocation slip within the adjacent grains [101-103] and these dislocations pass through the grains without hindrance because the grain size is sufficiently small that it is not possible to form subgrains [104].

It is feasible to model the flow by GBS in superplasticity and this leads to an equation in the conventional form for the rate of flow under steady-state conditions, $\dot{\varepsilon}$:

$$\dot{\varepsilon} = \frac{ADG\mathbf{b}}{kT}\left(\frac{\mathbf{b}}{d}\right)^{p}\left(\frac{\sigma}{G}\right)^{n} \qquad (1)$$

where D is the appropriate diffusion coefficient, G is the shear modulus, **b** is the Burgers vector, k is Boltzmann's constant, T is the absolute temperature, d is the grain size, σ is the applied stress, p and n are the exponents of the inverse grain size and the stress, respectively, and A is a dimensionless constant [105]. In the theoretical model for GBS, $D = D_{o(gb)} \exp(-Q_{gb}/kT)$ for

the coefficient for grain boundary diffusion where $D_{o(gb)}$ is the frequency factor and Q_{gb} is the activation energy for grain boundary diffusion, $p = 2$, $n = 2$ and $A = 10$ [105]. Several analyses have shown that eq. (1) is consistent with the rates of superplastic flow in numerous Al and Mg alloys after processing by ECAP or HPT [106-109].

In order to check the applicability of eq. (1) to the many superplastic results now available for the various Al-Mg-Sc alloys, similar analyses were conducted using the experimental data available in Tables 1, 2, 3 and 4. As in the earlier analyses [106-109], these analyses were performed using basic parameters for pure Al where $D_{o(gb)} = 1.86 \times 10^{-4}$ m^2 s^{-1} [110], $Q_{gb} = 86$ kJ mol^{-1} [110], $\mathbf{b} = 2.86 \times 10^{-10}$ m [110] and $G = 3.022 \times 10^4 - 16T$ MPa with the temperature expressed in degrees Kelvin [110].

Using eq. (1), the temperature and grain size compensated strain rate was plotted against the normalized stress as shown in Fig. 4 for results obtained without processing by SPD as listed in Table 1 [32-37,39-48], in Fig. 5 for results obtained after ECAP as listed in Table 2 [50,52-54,56,59-67,69,72,74,75,77-79], in Fig. 6 for results obtained after HPT as listed in Table 3 [66,80,82,83,79] and in Fig. 7 for results obtained after FSP as listed in Table 4 [84-90]. In each plot, the line labelled $\dot{\varepsilon}_{sp}$ corresponds to the theoretical prediction of the rate of superplasticity in conventional superplastic materials.

Several conclusions may be drawn from inspection of Figs 4-7.

First, all of the results are mutually consistent. Although the analyses are based on more than forty different publications documenting data obtained in laboratories in many different countries, all results lie together to within less than one order of magnitude of strain rate.

Second, the precise chemical compositions of the alloy play no significant role in affecting the rate of superplastic flow even though there is recent evidence for significant precipitation in severely deformed Al-Mg alloys [111,112]. Thus, inspection of Tables 1-4

shows that there are large variations in the compositions of the various alloys with the Mg composition varying between 1 and 6%, the Sc content varying from 0.1 to 0.5% and with various additions of Zn, Cu, Mn, Zr and other elements. Nevertheless, all of the datum points are mutually consistent with no clear dependence on composition.

Third, there is a general consistency with the predicted stress exponent of $n = 2$. Although the results without SPD and after ECAP and HPT tend to lie below the predicted line for conventional superplasticity, the points are generally consistent with the predicted behavior to within one order of magnitude of strain rate and they suggest a stress exponent close to ~2. It is surprising to note that the results with the FSP specimens are in even better agreement with the theoretical model despite the inhomogeneities that are an inherent feature of these samples.

From this comprehensive analysis, it is therefore reasonable to conclude that the theoretical relationship developed originally for superplasticity in conventional alloys provides also an excellent prediction for the superplastic behavior of Al-Mg-Sc alloys prepared both without and with SPD processing.

VI. SUMMARY AND CONCLUSIONS

1. The Al-Mg-Sc alloys are excellent candidate materials for exhibiting high superplastic elongations when testing in tension at elevated temperatures. Results are now available for a very large number of Al-Mg-Sc alloys and these various results were tabulated according to whether the materials were processed without the use of any SPD technique, with SPD processing in the form of ECAP or HPT and through processing by FSP.

2. Analysis of the data shows that all results are mutually consistent and the rate of superplastic flow has no significant dependence on the precise chemical composition of the alloy.

3. The results confirm a stress exponent of $n = 2$ as predicted by the theoretical model for superplasticity in conventional materials and the various experimental results are

generally consistent with the theoretical model to within less than one order of magnitude of strain rate.

ACKNOWLEDGEMENTS

This work was supported in part by the NRF Korea funded by MoE under Grant No. NRF-2016R1A6A1A03013422 and by MSIP under Grant No. NRF-2016K1A4A3914691, in part by the National Science Foundation of the United States under Grant No. DMR-1160966 and in part by the European Research Council under ERC Grant Agreement No. 267464-SPDMETALS.

REFERENCES

1. C.E. Pearson: The viscous properties of extruded eutectic alloys of lead-tin and bismuth-tin. *J. Inst. Metals* **54**, 111 (1934).
2. A.J. Barnes: Superplastic forming 40 years and still growing. *J. Mater. Eng. Perform.* **16**, 440 (2007).
3. T.G. Langdon: The mechanical properties of superplastic materials. *Metall. Trans.* **13A**, 689 (1982).
4. R.Z. Valiev, O.A. Kaibyshev, R.I. Kuznetsov, R.Sh. Musalimov, N.K. Tsenev: Low-temperature superplasticity of metallic materials. *Doklady Akad. Nauk SSSR* **301**, 864 (1988).
5. R.Z. Valiev, R.K. Islamgaliev, and I.V. Alexandrov: Bulk nanostructured materials from severe plastic deformation. *Prog. Mater. Sci*. **45**, 103 (2000).
6. R.Z. Valiev, Y. Estrin, Z. Horita, T.G. Langdon, M.J. Zehetbauer, and Y.T. Zhu: Producing bulk ultrafine-grained materials by severe plastic deformation. *JOM* **58**(4), 33 (2006).
7. T.G. Langdon: Twenty-five years of ultrafine-grained materials: Achieving exceptional properties through grain refinement. *Acta Mater.* **61**, 7035 (2013).
8. R.Z. Valiev and T.G. Langdon: Principles of equal-channel angular pressing as a processing tool for grain refinement. *Prog. Mater. Sci.* **51**, 881 (2006).
9. A.P. Zhilyaev and T.G. Langdon: Using high-pressure torsion for metal processing: Fundamentals and applications. *Prog. Mater. Sci.* **53**, 893 (2008).
10. A.P. Zhilyaev, G.V. Nurislamova, B.K. Kim. M.D. Baró, J.A. Szpunar, and T.G. Langdon: Experimental parameters influencing grain refinement and microstructural evolution during high-pressure torsion. *Acta Mater.* **51**, 753 (2003).

11. J. Wongsa-Ngam, M. Kawasaki, and T.G. Langdon: A comparison of microstructures and mechanical properties in a Cu-Zr alloy processed using different SPD techniques. *J. Mater. Sci.* **48**, 4653 (2013).
12. Y. Iwahashi, Z. Horita, M. Nemoto, and T.G. Langdon: An investigation of microstructural evolution in equal-channel angular pressing. *Acta Mater.* **45**, 4733 (1997).
13. Y. Iwahashi, Z. Horita, M. Nemoto, and T.G. Langdon: The process of grain refinement in equal-channel angular pressing. *Acta Mater.* **46**, 3317 (1998).
14. K.T. Park, H.J. Lee, C.S. Lee, and D.H. Shin: Effect of post-rolling after ECAP on deformation behavior of ECAPed commercial Al-Mg alloy at 723 K. *Mater. Sci. Eng. A* **393**, 118 (2005).
15. H.J. Lee, J.K. Han, S. Janakiraman, B. Ahn, M. Kawasaki, and T.G. Langdon: Significance of grain refinement on microstructure and mechanical properties of an Al-3% Mg alloy processed by high-pressure torsion. *Mater. Sci. Eng. A* **393**, 118 (2005).
16. Y. Iwahashi, Z. Horita, M. Nemoto, and T.G. Langdon: Factors influencing the equilibrium grain size in equal-channel angular pressing: Role of Mg additions to aluminum. *Metall. Mater. Trans. A* **29A**, 2503 (1998).
17. J. Wang, Y. Iwahashi, Z. Horita, M. Furukawa, M. Nemoto, R.Z. Valiev, and T.G. Langdon: An investigation of microstructural stability in an Al-Mg alloy with submicrometer grain size. *Acta Mater.* **44**, 2973 (1996).
18. J. Wang, M. Furukawa, M. Nemoto, Z. Horita, R.Z. Valiev, and T.G. Langdon: Enhanced grain growth in an Al-Mg alloy with ultrafine grain size. *Mater. Sci. Eng. A* **216**, 41 (1996).
19. M. Furukawa, Y. Iwahashi, Z. Horita, M. Nemoto, R.Z. Valiev, N.K. Tsenev, and T.G. Langdon: Structural evolution and the Hall-Petch relationship in an Al-Mg-Li-Zr alloy with ultra-fine grain size. *Acta Mater.* **45**, 4751 (1997).

20. H. Hasegawa, S. Komura, A. Utsunomiya, Z. Horita, M. Furukawa, M. Nemoto, and T.G. Langdon: Thermal stability of ultrafine-grained aluminum in the presence of Mg and Zr additions. *Mater. Sci. Eng. A* **265**, 188 (1999).
21. A. Yamashita, D. Yamaguchi, Z. Horita, and T.G. Langdon: Influence of pressing temperature on microstructural development in equal-channel angular pressing. *Mater. Sci. Eng. A* **287**, 100 (2000).
22. E. Avtokratova, O. Sitdikov, O. Mukhametdinova, M. Markushev, S.V.S. Narayana Murty, M.J.N.V. Prasad, and B.P. Kashyap. Microstructural evolution in Al-Mg-Sc-Zr alloy during severe plastic deformation and annealing. *J. Alloys Compds* **673**, 182 (2016).
23. D.A. Woodford: Strain-rate sensitivity as a measure of ductility. *Trans. Am. Soc. Metals* **62**, 291 (1969).
24. T.G. Langdon: The relationship between strain rate sensitivity and ductility in superplastic materials. *Scr. Metall.* **11**, 997 (1977).
25. F.A. Mohamed and T.G. Langdon: The transition from dislocation climb to viscous glide in creep of solid solution alloys. *Acta Metall.* **22**, 779 (1974).
26. P. Yavari and T.G. Langdon: An examination of the breakdown in creep by viscous glide in solid solution alloys at high stress levels. *Acta Metall.* **30**, 2181 (1982).
27. F.A. Mohamed: Creep ductility in large-grained solid solution alloys. *Scr. Metall.* **12**, 99 (1978).
28. P.E. Krajewski and J.G. Schroth: Overview of quick plastic forming technology. *Mater. Sci. Forum* **551-552**, 3 (2007).
29. E.M. Taleff, D.R. Lesuer, and J. Wadsworth: Enhanced ductility in coarse-grained Al-Mg alloys. *Metall. Mater. Trans. A* **27A**, 343 (1996).
30. T.G. Langdon: Seventy-five years of superplasticity: Historic developments and new opportunities. *J. Mater. Sci.* **44**, 5998 (2009).

31. M. Otsuka, S. Shibasaki, and M. Kikuchi: Superplasticity in coarse grained Al-Mg alloys. *Mater. Sci. Forum* **233-234**, 193 (1997).

32. R.R. Sawtell and C.L. Jensen: Mechanical properties and microstructures of Al-Mg-Sc alloys. *Metall. Mater. Trans. A* **21A**, 421 (1990).

33. T.G. Nieh, L.M. Hsiung, J. Wadsworth, and R. Kaibyshev: High strain rate superplasticity in a continuously recrystallized Al-6%Mg-0.3%Sc alloy. *Acta Mater*. **46**, 2789 (1998).

34. R. Kaibyshev, E. Avtokratova, A. Apollonov, and R. Davies: High strain rate superplasticity in an Al-Mg-Sc-Zr alloy subjected to simple thermomechanical processing. Scr. *Mater*. **54**, 2119 (2006).

35. Y.Y. Peng, Z.M. Yin, B. Nie, and L. Zhong: Effect of minor Sc and Zr on superplasticity of Al-Mg-Mn alloys. *Trans. Nonferrous Met. Soc. China* **17**, 744 (2007).

36. A. Kumar, A.K. Mukhopadhyay, and K.S. Prasad: Superplastic behaviour of Al-Zn-Mg-Cu-Zr alloy AA7010 containing Sc. *Mater. Sci. Eng. A* **527**, 854 (2010).

37. A. Smolej, B. Skaza, and V. Dragojević: Superplastic behavior of Al-4.5Mg-0.46Mn-0.44Sc alloy sheet produced by a conventional rolling process. *J. Mater. Eng. Perform* **19**, 221 (2010).

38. A.K. Mukhopadhyay, A. Kumar, S. Raveendra, and I. Samajdar: Development of grain structure during superplastic deformation of an Al-Zn-Mg-Cu-Zr alloy containing Sc. *Scr. Mater.* **64**, 386 (2011).

39. X. Cao, G. Xu, Y. Duan, Z. Yin, L. Lu, and Y. Wang: Achieving high superplasticity of a new Al-Mg-Sc-Zr alloy sheet prepared by a simple thermal-mechanical process. *Mater. Sci. Eng. A* **647**, 333 (2015).

40. Y. Duan, G. Xu, L. Zhou, D. Xiao, Y. Deng, Z. Yin, B. Peng, Q. Pan, Y. Wang, and L. Lu: Achieving high superplasticity of a traditional thermal-mechanical processed non-superplastic Al-Zn-Mg alloy sheet by low Sc additions. *J. Alloys Comp.* **638**, 364 (2015).

41. Y.I. Duan, G.F. Xu, D. Xiao, L.Q. Zhou, Y. Deng, and Z.M. Yin: Excellent superplasticity and deformation mechanism of Al-Mg-Sc-Zr alloy processed via simple free forging. *Mater. Sci. Eng. A* **624**, 124 (2015).
42. Y.I. Duan, G.F. Xu, X.Y. Peng, Y. Deng, Z. Li, and Z.M. Yin: Effect of Sc and Zr additions on grain stability and superplasticity of the simple thermal-mechanical processed Al-Zn-Mg alloy sheet. *Mater. Sci. Eng. A* **648**, 80 (2015).
43. A.D. Kotov, A.V. Mikhaylovskaya, M.S. Kishchik, A.A. Tsarkov, S.A. Aksenov, and V.K. Portnoy: Superplasticity of high-strength Al-based alloys produced by thermomechanical treatment. *J. Alloys Comp.* **688**, 336 (2016).
44. A.V. Mikhaylovskaya, O.A. Yakovtseva, V.V. Cheverikin, A.D. Kotov, and V.K. Portnoy: Superplastic behaviour of Al-Mg-Zn-Zr-Sc-based alloys at high strain rates. *Mater. Sci. Eng. A* **659**, 225 (2016).
45. X. Sun, Q. Pan, M. Li, Y. Shi, and J. Yan: Superplastic deformation behavior of cold-rolled Al-Mg-Sc-Zr alloy. *Chinese J. Nonferr. Metal.* **26**, 280 (2016).
46. G. Xu, X. Cao, T. Zhang, Y. Duan, X. Peng, Y. Deng, and Z. Yin: Achieving high strain rate superplasticity of an Al-Mg-Sc-Zr alloy by a new asymmetrical rolling technology. *Mater. Sci. Eng. A* **672**, 98 (2016).
47. H. Xiang, Q.L. Pan, X.H. Yu, X. Huang, X. Sun, X.D. Wang, M.J. Li, and Z.M. Yin: Superplasticity behaviors of Al-Zn-Mg-Zr cold-rolled alloy sheet with minor Sc addition. *Mater. Sci. Eng. A* **676**, 128 (2016).
48. M. Li, Q. Pan, Y. Shi, X. Sun, and H. Xiang: High strain rate superplasticity in an Al-Mg-Sc-Zr alloy processed via simple rolling. *Mater. Sci. Eng. A* **687**, 298 (2017).
49. S. Komura, P.B. Berbon, M. Furukawa, Z. Horita, M. Nemoto, and T.G. Langdon: High strain rate superplasticity in an Al-Mg alloy containing scandium. *Scr. Mater.* **38**, 1851 (1998).

50. Z. Horita, M. Furukawa, M. Nemoto, A.J. Barnes and T.G. Langdon: Superplastic forming at high strain rates after severe plastic deformation. *Acta Mater.* **48**, 3633 (2000).

51. S. Komura, Z. Horita, M. Furukawa, M. Nemoto, and T.G. Langdon: Influence of scandium on superplastic ductilities in an Al-Mg-Sc alloy. *J. Mater. Res.* **15**, 2571 (2000).

52. H. Akamatsu, T. Fujinami, Z. Horita, and T.G. Langdon: Influence of rolling on the superplastic behavior of an Al-Mg-Sc alloy after ECAP. *Scr. Mater.* **44**, 759 (2001).

53. M. Furukawa, A. Utsunomiya, K. Matsubara, Z. Horita, and T.G. Langdon: Influence of magnesium on grain refinement and ductility in a dilute Al-Sc alloy. *Acta Mater.* **49**, 3829 (2001).

54. S. Komura, Z. Horita, M. Furukawa, M. Nemoto, and T.G. Langdon: An evaluation of the flow behavior during high strain rate superplasticity in an Al-Mg-Sc alloy. *Metall. Mater. Trans. A* **32A**, 707 (2001).

55. S. Komura, M. Furukawa, Z. Horita, M. Nemoto, and T.G. Langdon: Optimizing the procedure of equal-channel angular pressing for maximum superplasticity. *Mater. Sci. Eng. A* **297**, 111 (2001).

56. S. Lee, A. Utsunomiya, H. Akamatsu, K. Neishi, M. Furukawa, Z. Horita, and T.G. Langdon: Influence of scandium and zirconium on grain stability and superplastic ductilities in ultrafine-grained Al–Mg alloys. *Acta Mater.* **50**, 553 (2002).

57. V.N. Perevezentsev, V.N. Chuvil'deev, V.I. Kopylov, A.N. Sysoev, and T.G. Langdon: Developing high strain rate superplasticity in Al-Mg-Sc-Zr alloys using equal-channel angular pressing. *Ann. Chim. Sci. Mat.* **27**, 99 (2002).

58. S. Ota, H. Akamatsu, K Neishi, M. Furukawa, Z. Horita, and T.G. Langdon: Low-temperature superplasticity in aluminium alloys processed by equal-channel angular pressing. *Mater. Trans.* **43**, 2364 (2002).

59. V.N. Perevezentsev, V.N. Chuvil'deev, A.N. Sysoev, V.I. Kopylov, and T.G. Langdon: Achieving high-strain-rate superplasticity in Al-Mg-Sc-Zr alloys after severe plastic deformation. *Phys. Met. Metallogr.* **94**, S45 (2002).

60. R.K. Islamgaliev, N.F. Yunusova, R.Z. Valiev, N.K. Tsenev, V.N. Perevezentsev, and T.G. Langdon: Characteristics of superplasticity in an ultrafine-grained aluminum alloy processed by ECA pressing. *Scr. Mater.* **49**, 467 (2003).

61. F. Musin, R. Kaibyshev, Y. Motohashi, and G. Itoh: High strain rate superplasticity in a commercial Al-Mg-Sc alloy. *Scr. Mater.* **50**, 511 (2004).

62. V.N. Perevezentsev, V.N. Chuvil'deev, V.I. Kopylov, A.N. Sysoev, and T.G. Langdon: High-strain-rate superplasticity of Al-Mg-Sc-Zr alloys. *Russ. Metall. (Metally)* **1**, 28 (2004).

63. M. Kamachi, M. Furukawa, Z. Horita, and T.G. Langdon: Achieving superplasticity of Al-1%Mg-0.2%Sc alloy in plate samples processed by equal channel angular pressing. *Mater. Trans.* **45**, 2521 (2004).

64. K.-T. Park, H.-J. Lee, C.S. Lee, W.J. Nam, and D.H. Shin: Enhancement of high strain rate superplastic elongation of a modified 5154 Al by subsequent rolling after equal channel angular pressing. *Scr. Mater.* **51**, 479 (2004).

65. G. Sakai, Z. Horita, and T.G. Langdon: An evaluation of superplastic anisotropy after processing by equal-channel angular pressing. *Mater. Trans.* **45**, 3079 (2004).

66. G. Sakai, Z. Horita, and T.G. Langdon: Grain refinement and superplasticity in an aluminum alloy processed by high-pressure torsion. *Mater. Sci. Eng. A* **393**, 344 (2005).

67. R. Kaibyshev, K. Shipilova, F. Musin, and Y. Motohashi: Achieving high strain rate superplasticity in an Al-Li-Mg alloy through equal channel angular extrusion. *Mater. Sci. Tech.* **21**, 408 (2005).

68. P. Málek, K. Turba, M. Cieslar, I. Drbohlav, and T. Kruml: Structure development during superplastic deformation of an Al-Mg-Sc-Zr alloy produced by equal-channel angular pressing. *Mater. Sci. Eng. A* **462**, 95 (2007).
69. K. Turba, P. Málek, and M. Cieslar: Superplasticity in an Al-Mg-Zr-Sc alloy produced by equal-channel angular pressing. *Mater. Sci. Eng. A* **462**, 91 (2007).
70. E. Avtokratova, O. Sitdikov, M. Markushev, and R. Mulyukov: Extraordinary high-strain rate superplasticity of severely deformed Al-Mg-Sc-Zr alloy. *Mater. Sci. Eng. A* **538**, 386 (2012).
71. E. Avtokratova, O. Sitdikov, O. Mukhametdinova, and M. Markushev: High strain rate superplasticity in an Al-Mg-Sc-Zr alloy produced by equal channel angular pressing and subsequent cold and warm rolling. *Mater. Sci. Forum* **710**, 223 (2012).
72. R. Kaibyshev, D. Zhemchuzhnikova, and A. Mogucheva: Effect of Mg content on high strain rate superplasticity of Al-Mg-Sc-Zr alloys subjected to equal-channel angular pressing. *Mater. Sci. Forum* **735**, 265 (2013).
73. E. Avtokratova, O. Sitdikov, and M. Markushev: Effect of cold/warm rolling following warm ECAP on superplastic properties of an Al-5.8%Mg-0.32%Sc alloy. *Lett. Mater*. **5**, 319 (2015).
74. A. Dubyna, S. Malopheyev, and R. Kaibyshev: Effect of rolling on superplastic behavior of an Al-Mg-Sc alloy with ultrafine-grained structure. *Mater. Sci. Forum* **838-839**, 416 (2016).
75. A. Mogucheva, D. Yuzbekova, and R. Kaibyshev: Superplasticity in a 5024 aluminium alloy subjected to ECAP and subsequent cold rolling. *Mater. Sci. Forum* **838-839**, 428 (2016).
76. D. Yuzbekova, A. Mogucheva, and R. Kaibyshev: Low-temperature superplasticity in an Al-Mg-Sc alloy processed by ECAP. *Mater. Sci. Forum* **838-839**, 422 (2016).

77. D. Yuzbekova, A. Mogucheva, and R. Kaibyshev: Superplasticity of ultrafine-grained Al-Mg-Sc-Zr alloy. *Mater. Sci. Eng. A* **675**, 228 (2016).

78. P.H.R. Pereira, Y.C. Wang, Y. Huang, and T.G. Langdon: Influence of grain size on the flow properties of an Al-Mg-Sc alloy over seven orders of magnitude of strain rate. *Mater. Sci. Eng. A* **685**, 367 (2017).

79. P.H.R. Pereira, Y. Huang, and T.G. Langdon: Thermal stability and superplastic behaviour of an Al-Mg-Sc alloy processed by ECAP and HPT at different temperatures. *IOP Conf. Ser. Mater. Sci. Eng.* (2017); in press.

80. V.N. Perevezentsev, M.Y. Shcherban, M.Y. Murashkin, and R.Z. Valiev: High-strain-rate superplasticity of nanocrystalline aluminum alloy 1570. *Tech. Phys. Lett.* **33**, 648 (2007).

81. Z. Horita and T.G. Langdon: Achieving exceptional superplasticity in a bulk aluminum alloy processed by high-pressure torsion. *Scr. Mater.* **58**, 1029 (2008).

82. Y. Harai, K. Edalati, Z. Horita, and T.G. Langdon: Using ring samples to evaluate the processing characteristics in high-pressure torsion. *Acta Mater.* **57**, 1147 (2009).

83. P.H.R. Pereira, Y. Huang, and T.G. Langdon: Examining the mechanical properties and superplastic behaviour in an Al-Mg-Sc alloy after processing by HPT. *Lett. Mater.* **5**, 294 (2015).

84. I. Charit and R.S. Mishra: Low temperature superplasticity in a friction-stir-processed ultrafine grained Al-Zn-Mg-Sc alloy. *Acta Mater.* **53**, 4211 (2005).

85. F.C. Liu and Z.Y. Ma: Achieving exceptionally high superplasticity at high strain rates in a micrograined Al–Mg–Sc alloy produced by friction stir processing. *Scr. Mater.* **59**, 882 (2008).

86. F.C. Liu, Z.Y. Ma, and L.Q. Chen: Low-temperature superplasticity of Al-Mg-Sc alloy produced by friction stir processing. *Scr. Mater.* **60**, 968 (2009).

87. F.C. Liu and Z.Y. Ma: Contribution of grain boundary sliding in low-temperature superplasticity of ultrafine-grained aluminum alloys. *Scr. Mater.* **62**, 125 (2010).

88. F.C. Liu, Z.Y. Ma, and F.C. Zhang: High strain rate superplasticity in a micro-grained Al-Mg-Sc alloy with predominant high angle grain boundaries. *J. Mater. Sci. Technol.* **28**, 1025 (2012).

89. A. Smolej, D. Klobčar, B. Skaza, A. Nagode, E. Slaček, V. Dragojević, and S. Smolej: Superplasticity of the rolled and friction stir processed Al-4.5Mg-0.35Sc-0.15Zr alloy. *Mater. Sci. Eng. A* **590**, 239 (2014).

90. A. Smolej, D. Klobčar, B. Skaza, A. Nagode, E. Slaček, V. Dragojević, and S. Smolej: The superplasticity of friction stir processed Al-5Mg alloy with additions of scandium and zirconium. *Int. J. Mater. Res.* **105**, 1218 (2014).

91. Z.Y. Ma: Friction stir processing technology: A review. *Metall. Mater. Trans. A* **39A**, 642 (2008).

92. X. He, F. Gu, and A. Ball: A review of numerical analysis of friction stir welding. *Prog. Mater. Sci.* **65**, 1 (2014).

93. Y. Iwahashi, J. Wang, Z. Horita, M. Nemoto, and T.G. Langdon. Principle of equal-channel angular pressing for the processing of ultra-fine grained materials. *Scr. Mater.* **35**, 143 (1996).

94. M. Kamachi, M. Furukawa, Z. Horita, and T.G. Langdon: Equal-channel angular pressing using plate samples. *Mater. Sci. Eng. A* **361**, 258 (2003).

95. Y. Takizawa, T. Masuda, K. Fujimitsu, T. Kajita, K. Watanabe, M. Yumoto, Y. Otagiri, and Z. Horita: Scaling up of high-pressure sliding (HPS) for grain refinement and superplasticity. *Metall. Mater. Trans. A* **47A**, 4669 (2016)

96. Y.H. Zhao, Y.Z. Guo, Q. Wei, A.M. Dangelewicz, C. Xu, Y.T. Zhu, T.G. Langdon, Y.Z. Zhou, and E.J. Lavernia: Influence of specimen dimensions on the tensile behavior of ultrafine-grained Cu. *Scr. Mater.* **59**, 627 (2008).

97. Y.H. Zhao, Y.Z. Guo, Q. Wei, T.D. Topping, A.M. Dangelewicz, Y.T. Zhu, T.G. Langdon, and E.J. Lavernia: Influence of specimen dimensions and strain measurement methods on tensile stress-strain curves. *Mater. Sci. Eng. A* **525**, 68 (2009).

98. R.Z. Valiev, D.A. Salimonenko, N.K. Tsenev, P.B. Berbon, and T.G. Langdon: Observations of high strain rate superplasticity in commercial aluminum alloys with ultrafine grain sizes. *Scr. Mater.* **37**, 1945 (1997).

99. K. Higashi, M. Mabuchi, and T.G. Langdon: High-strain-rate superplasticity in metallic materials and the potential for ceramic materials. *ISIJ Intl.* **36**, 1423 (1996).

100. T.G. Langdon: An evaluation of the strain contributed by grain boundary sliding in superplasticity. *Mater. Sci. Eng. A* **174**, 225 (1994).

101. L.K.L. Falk, P.R. Howell, G.L. Dunlop, and T.G. Langdon: The role of matrix dislocations in the superplastic deformation of a copper alloy. *Acta Metall.* **34**, 1203 (1986).

102. R.Z. Valiev and T.G. Langdon, An investigation of the role of intragranular dislocation strain in the superplastic Pb-62% Sn eutectic alloy. *Acta Metall. Mater.* **41**, 949 (1993).

103. Y. Xun and F.A. Mohamed, Slip-accommodated superplastic flow in Zn-22 wt% Al. *Phil. Mag.* **83**, 2247 (2003).

104. F.A. Mohamed and T.G. Langdon: Deformation mechanism maps for superplastic materials. *Scr. Metall.* **10**, 759 (1976).

105. T.G. Langdon: A unified approach to grain boundary sliding in creep and superplasticity. *Acta Metall. Mater.* **42**, 2437 (1994).

106. M. Kawasaki and T.G. Langdon: Principles of superplasticity in ultrafine-grained materials. *J. Mater. Sci.* **42**, 1782 (2007).

107. M. Kawasaki, N. Balasubramanian, and T.G. Langdon: Flow mechanisms in ultrafine-grained metals with an emphasis on superplasticity. *Mater. Sci. Eng. A* **528**, 6624 (2011).
108. M. Kawasaki and T.G. Langdon: Review: Achieving superplasticity in metals processed by high-pressure torsion. *J. Mater. Sci.* **49**, 6487 (2014).
109. M. Kawasaki and T.G. Langdon, Review: Achieving superplastic properties in ultrafine-grained materials at high temperatures. *J. Mater. Sci.* **51**, 19 (2016).
110. F.A. Mohamed and T.G. Langdon: Deformation mechanism maps based on grain size. *Metall. Trans.* **5**, 2339 (1974).
111. X. Sauvage, N. Enikeev, R. Valiev, Y. Nasedkina, and M. Murashkin: Atomic-scale analysis of the segregation and precipitation mechanisms in a severely deformed Al-Mg alloy. *Acta Mater.* **72**, 125 (2014).
112. Yu. Buranova, V. Kulitskiy, M. Peterlechner, A. Mogucheva, R. Kaibyshev, S.V. Divinski, and G. Wilde: Al_3(Sc,Zr)-based precipitates in Al-Mg alloy: Effect of severe deformation. *Acta Mater.* **124**, 210 (2017).

Figure captions

FIG. 1 Examples of superplasticity in Al-3% Mg-0.2% Sc specimens after processing by ECAP or HPT.

FIG. 2 Elongation versus temperature of testing for various superplastic Al-Mg-Sc alloys from different processing routes: Cold-rolling [34,37,39,46], ECAP [54,67,70,76], HPT [80-82,79], FSP [84,85,88.89].

FIG. 3 Elongation versus initial strain rate for various superplastic Al-Mg-Sc alloys from different processing routes: Cold-rolling [34,37,39,46], ECAP [54,67,70,76], HPT [80-82,79], FSP [84,85,88.89].

FIG. 4 Temperature and grain size compensated strain rate versus normalized stress for various superplastic Al-Mg-Sc alloys without SPD processing [32-37,39-48]: the solid line shows the theoretical prediction for superplastic flow in conventional metals not processed using SPD techniques.

FIG. 5 Temperature and grain size compensated strain rate versus normalized stress for various superplastic Al-Mg-Sc alloys processed by ECAP [50,52-54,56,59-67,69,72,74,75,77-79]: the solid line shows the theoretical prediction for superplastic flow in conventional metals not processed using SPD techniques.

FIG. 6 Temperature and grain size compensated strain rate versus normalized stress for various superplastic Al-Mg-Sc alloys processed by HPT [66,80,82,83,79]: the solid line shows the theoretical prediction for superplastic flow in conventional metals not processed using SPD techniques.

FIG. 7 Temperature and grain size compensated strain rate versus normalized stress for various superplastic Al-Mg-Sc alloys processed by FSP [84-90]: the solid line shows the theoretical prediction for superplastic flow in conventional metals not processed using SPD techniques.

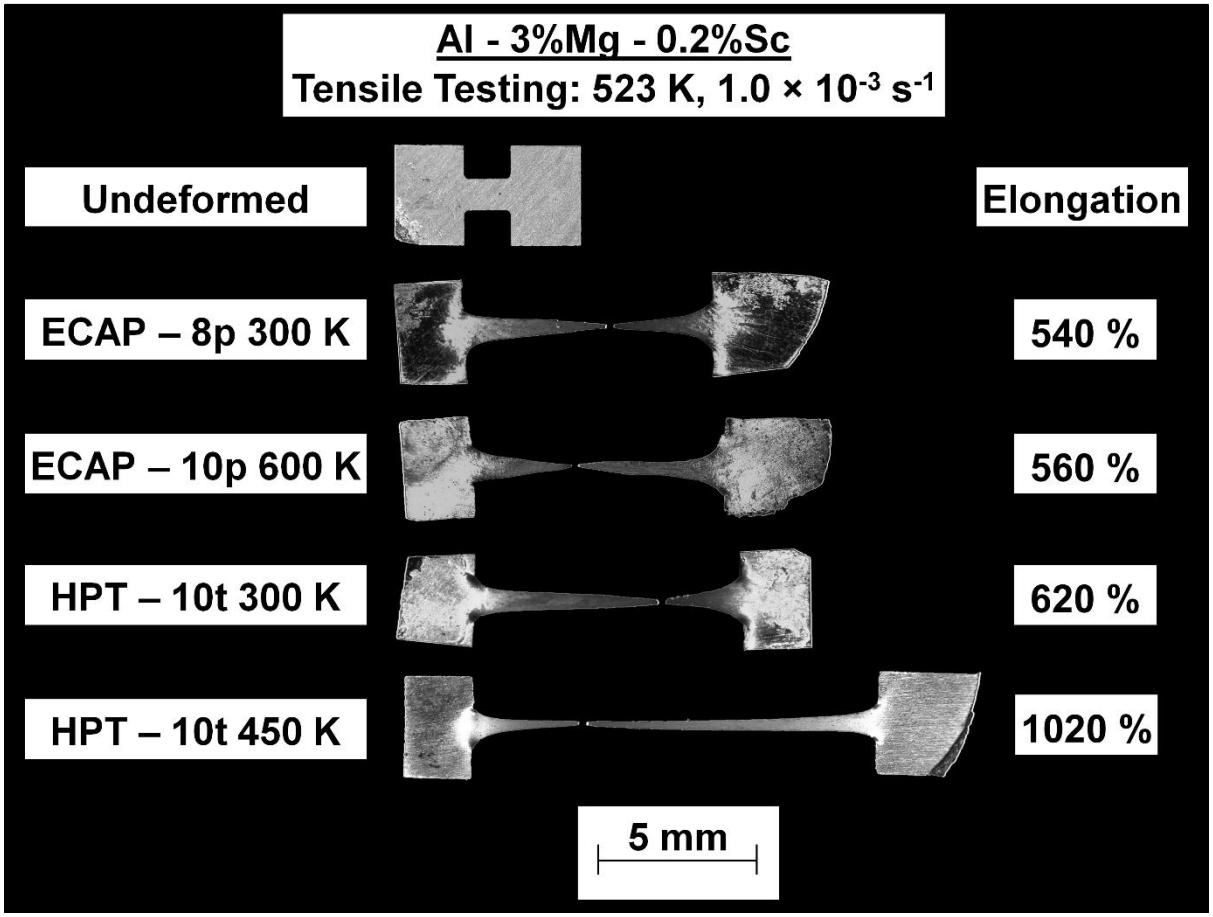

Fig.1 Examples of superplasticity in Al-3% Mg-0.2% Sc specimens after processing by ECAP or HPT.

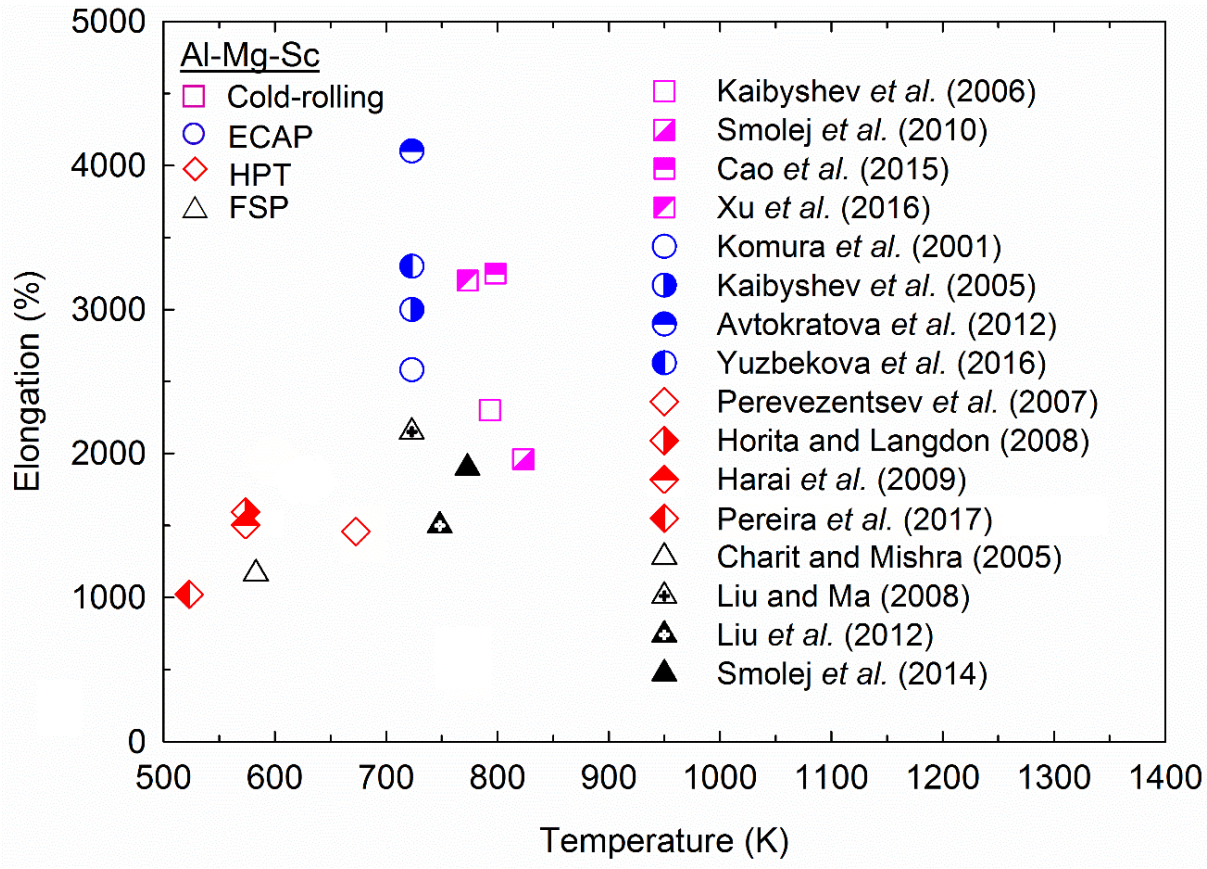

Fig. 2 Elongation versus temperature of testing for various superplastic Al-Mg-Sc alloys from different processing routes: Cold-rolling [34,37,39,46], ECAP [54,67,70,76], HPT [80-82,79], FSP [84,85,88.89].

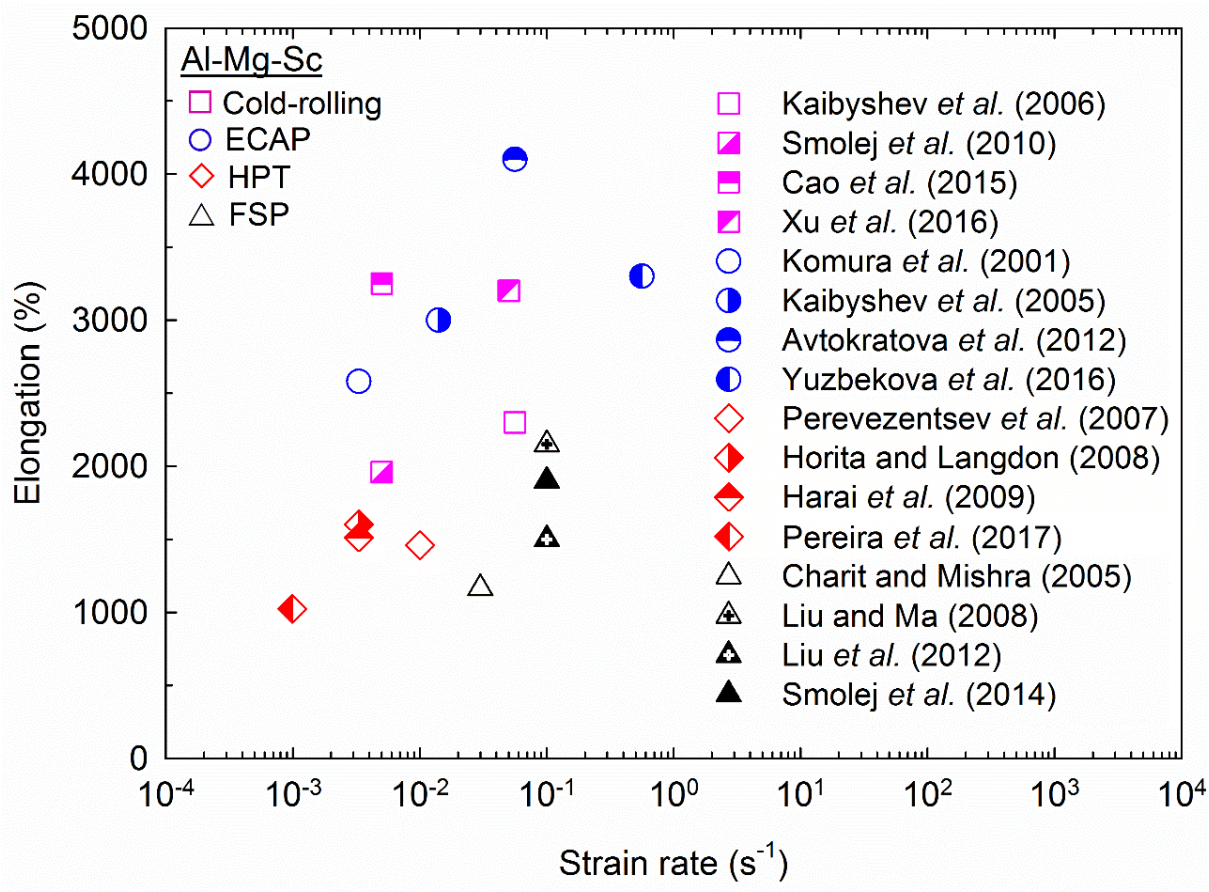

Fig. 3 Elongation versus initial strain rate for various superplastic Al-Mg-Sc alloys from different processing routes: Cold-rolling [34,37,39,46], ECAP [54,67,70,76], HPT [80-82,79], FSP [84,85,88.89].

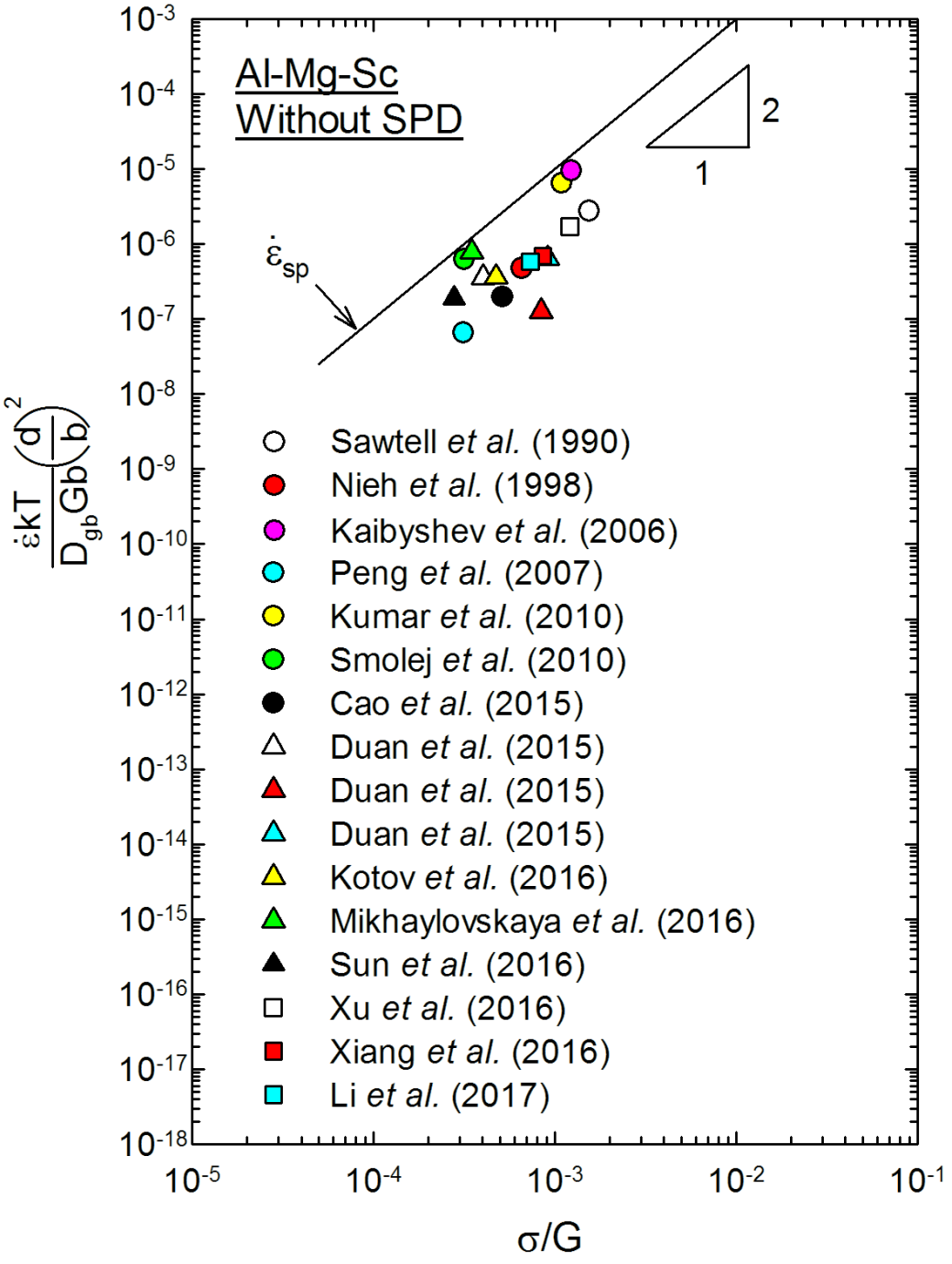

Fig. 4 Temperature and grain size compensated strain rate versus normalized stress for various superplastic Al-Mg-Sc alloys without SPD processing [32-37,39-48]: the solid line shows the theoretical prediction for superplastic flow in conventional metals not processed using SPD techniques.

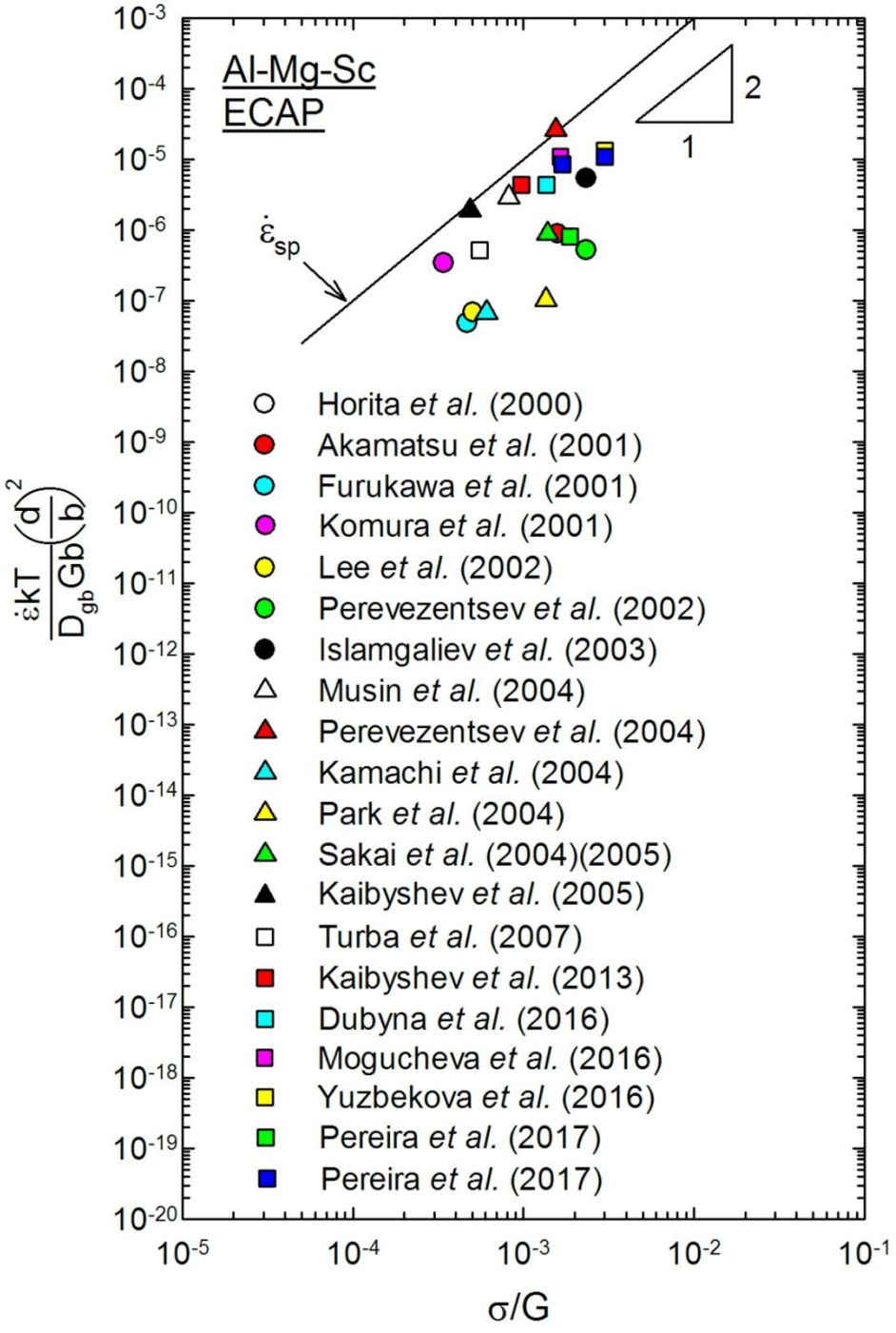

Fig. 5 Temperature and grain size compensated strain rate versus normalized stress for various superplastic Al-Mg-Sc alloys processed by ECAP [50,52-54,56,59-67,69,72,74,75,77-79]: the solid line shows the theoretical prediction for superplastic flow in conventional metals not processed using SPD techniques.

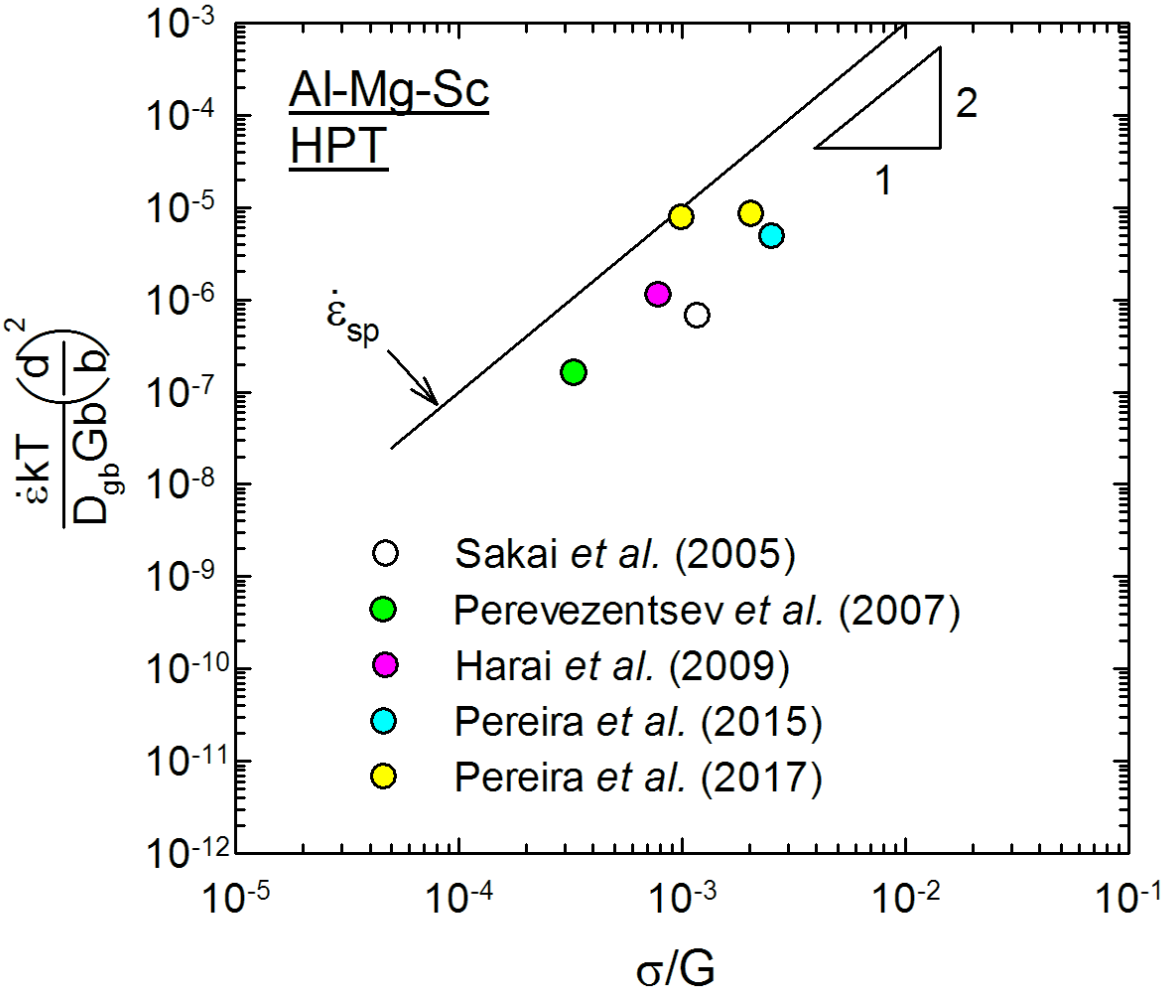

Fig. 6 Temperature and grain size compensated strain rate versus normalized stress for various superplastic Al-Mg-Sc alloys processed by HPT [66,80,82,83,79]: the solid line shows the theoretical prediction for superplastic flow in conventional metals not processed using SPD techniques.

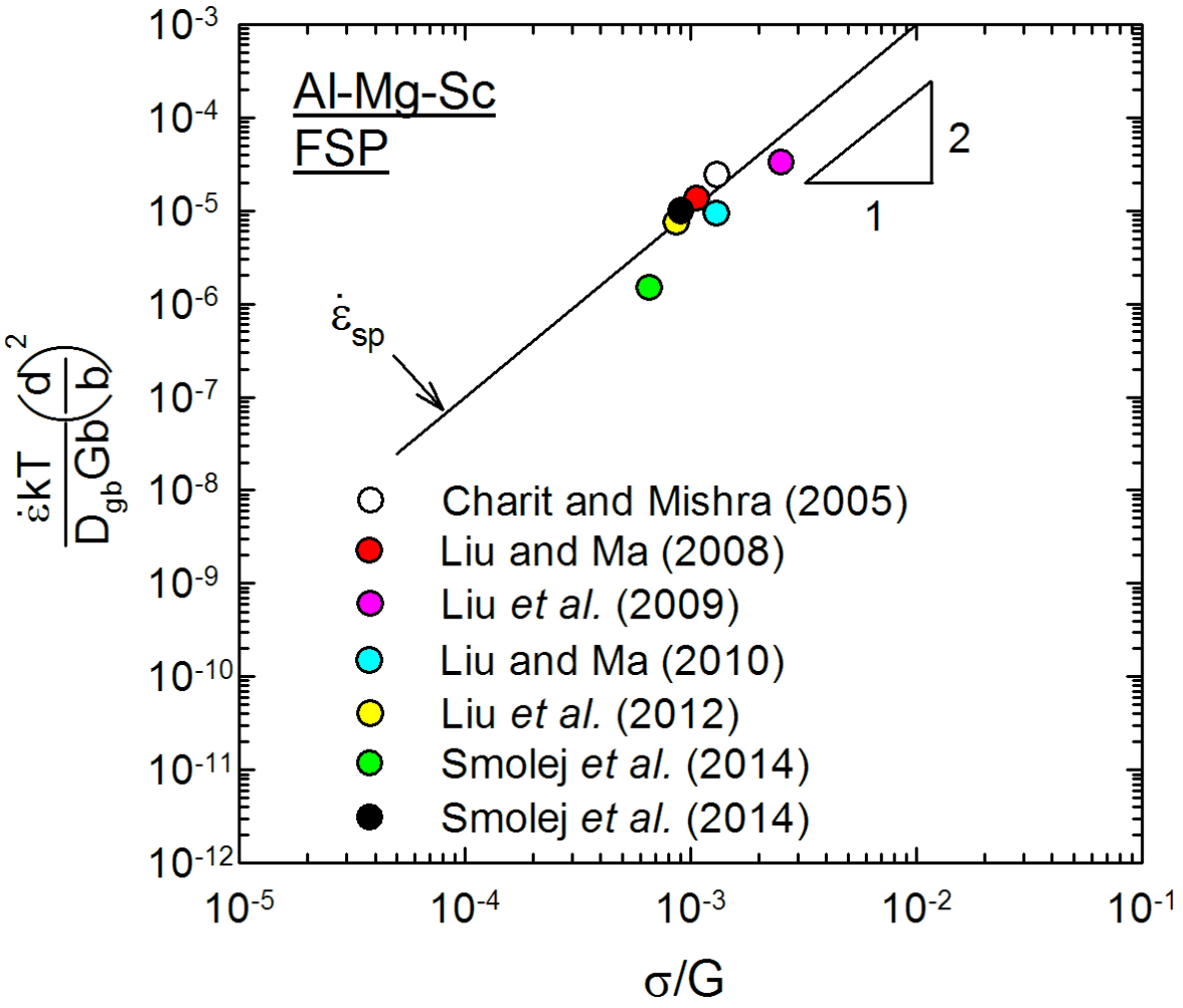

Fig. 7 Temperature and grain size compensated strain rate versus normalized stress for various superplastic Al-Mg-Sc alloys processed by FSP [84-90]: the solid line shows the theoretical prediction for superplastic flow in conventional metals not processed using SPD techniques.

Table 1

Reports of superplasticity in Al-Mg-Sc alloys without SPD processing.

Alloy or composition (wt.%)	Metal-working procedure	Grain size (μm)	Superplasticity			Reference
			Testing temperature (K)	Strain rate (s^{-1})	Maximum elongation (%)	
Al-4Mg-0.5Sc	Cold-rolling + Annealing at 672 K for 1h	~1 – 2	672	1.0×10^{-2}	>1020[a]	Sawtell *et al.* (1990) [32]
Al-5.76Mg-0.32Sc-0.3Mn	Cold-rolling + Annealing at 748 K for 45 min	~1	748	1.4×10^{-2}	1130	Nieh *et al.* (1998) [33]
Al-5Mg-0.2Sc-0.18Mn-0.08Zr	Cold-rolling	~5 – 15 [b]	793	5.6×10^{-2}	2300	Kaibyshev *et al.* (2006) [34]
Al-6.2Mg-0.4Mn-0.25Sc-0.12Zr	Cold-rolling	—	813	1.7×10^{-3}	690	Peng *et al.* (2007) [35]
Al-6.3Zn-2.3Mg-1.5Cu-0.23Sc-0.14Zr	Hot-rolling at 673 K	~10[b]	748	1.9×10^{-2}	650	Kumar *et al.* (2010) [36]
Al-4.5Mg-0.46Mn-0.44Sc	Cold-rolling + Annealing at 773 K for 2 h	~11	823	5.0×10^{-3}	1960	Smolej *et al.* (2010) [37]
Al-6.3Zn-2.3Mg-1.5Cu-0.23Sc-0.14Zr	Hot-rolling at 673 K	~2.4	698	$(10^{-1} + 10^{-2})$[c]	916	Mukhopadhyay *et al.* (2011) [38]
Al-6.1Mg-0.3Mn-0.25Sc-0.1Zr	Cold-rolling + Annealing at 573 K for 1 h	~2.5	798	5.0×10^{-3}	3250	Cao *et al.* (2015) [39]
Al-5.4Zn-1.9Mg-0.32Mn-0.25Cu-0.1Sc-0.1Zr	Cold-rolling + Solution treatment at 743 K for 1 h + Ageing at 393 K for 12 h	~3.1	773	5.0×10^{-3}	1050	Duan *et al.* (2015) [40]
Al-6.1Mg-0.3Mn-0.25Sc-0.1Zr	Free Forging	~3.7	748	1.0×10^{-3}	1590	Duan *et al.* (2015) [41]
Al-5.4Zn-1.9Mg-0.33Mn-0.32Cu-0.25Sc-0.1Zr	Cold-rolling + Solution treatment at 743 K for 1 h + Ageing at 393 K for 12 h	~2.8	773	1.0×10^{-2}	1520	Duan *et al.* (2015) [42]
Al-4.2Mg-3.7Zn-0.7Cu-0.2Zr-0.15Sc	Cold-rolling + Annealing at 693 K	~2	693	2.0×10^{-3}	800	Kotov *et al.* (2016) [43]
Al-Zn-Mg-0.2Zr-0.1Sc-Fe-Ni[d]	Cold-rolling + Annealing at 753 K for 20 min	~2.5	753	1.0×10^{-2}	915	Mikhaylovskaya *et al.* (2016) [44]
Al-5.8Mg-0.40Mn-0.25Sc-0.10Zr	Cold-rolling + Annealing at 672 K for 1h	~5 [b]	773	1.67×10^{-3}	740	Sun *et al.* (2016) [45]
Al-6.1Mg-0.3Mn-0.25Sc-0.1Zr	Asymmetrical rolling + Annealing at 573 K for 1 h	~1.5	773	5.0×10^{-2}	3200	Xu *et al.* (2016) [46]
Al-5.4Zn-2Mg-0.35Cu-0.3Mn-0.25Sc-0.1Zr	Cold-rolling	~3	773	1.0×10^{-2}	540	Xiang *et al.* (2016) [47]
Al-5.8Mg-0.4Mn-0.2Sc-0.1Zr (Al1570c)	Cold-rolling	~3.8[b]	773	6.7×10^{-3}	740	Li *et al.* (2017) [48]

[a] Maximum possible elongation detected by the tensile testing facility used in the referred study.
[b] Grain size in the gauge area after tensile testing.
[c] Tensile testing conducted at 1.0×10^{-1} s^{-1} up to a true strain of 0.73 and at 1.0×10^{-2} s^{-1} afterwards.
[d] The Mg, Zn, Ni and Fe contents in this alloy were not reported.

Table 2

Reports of superplasticity in Al-Mg-Sc alloys after ECAP.

Alloy or composition (wt.%)	ECAP processing				Metal-working procedure after ECAP	Grain size (μm)	Superplasticity			Reference
	Channel angle (°)	Processing temperature (K)	Processing route	Nº of passes			Testing temperature (K)	Strain rate (s^{-1})	Maximum elongation (%)	
Al-3Mg-0.2Sc	90	RT	B_c	8	—	~0.2	673	3.3×10^{-2}	1030	Komura *et al.* (1998) [49][a]
Al-3Mg-0.2Sc	90	RT	B_c	8	—	~0.2	673	3.3×10^{-2}	2280	Horita *et al.* (2000) [50]
Al-3Mg-0.2Sc	90	RT	B_c	8	—	~0.2	673	3.3×10^{-2}	950	Komura *et al.* (2000) [51][b]
Al-3Mg-0.2Sc	90	RT	B_c	8	Cold-rolling	~0.2[c]	673	3.3×10^{-2}	1860	Akamatsu *et al.*(2001) [52]
Al-1Mg-0.2Sc	90	RT	B_c	8	—	~0.36	673	1.0×10^{-3}	580	Furukawa *et al.* (2001) [53]
Al-3Mg-0.2Sc	90	RT	B_c	8	—	~0.2	723	3.3×10^{-3}	2580	Komura *et al.* (2001) [54]
Al-3Mg-0.2Sc	90	RT	A	8	—	—	673	3.3×10^{-2}	1170	Komura *et al.* (2001) [55]
Al-3Mg-0.2Sc	90	RT	C	8	—	—	673	3.3×10^{-2}	1370	Komura *et al.* (2001) [55]
Al-3Mg-0.2Sc-0.12Zr	90	RT	B_c	6	—	~0.3	773	1.0×10^{-2}	1680	Lee *et al.*(2002) [56]
Al-4.5Mg-0.22Sc-0.15Zr	90	448	B_c	6	—	~0.1	723	3.3×10^{-2}	2250	Perevezentsev *et al.* (2002) [57]
Al-3Mg-0.2Sc	90	RT	B_c	8	—	~0.2	523	3.3×10^{-4}	640	Ota *et al.* (2002) [58]
Al-1.5Mg-0.22Sc-0.15Zr	90	448	B_c	6 – 8[d]	—	~0.1	723	1.0×10^{-1}	1590	Perevezentsev *et al.* (2002) [59]
Al-5.5Mg-2.2Li-0.2Sc-0.12Zr (Al1421)	90	643	B_c	12	—	~0.3 – 0.4	673	1.0×10^{-1}	1500	Islamgaliev *et al.* (2003) [60]
Al-5.8Mg-0.3Mn-0.32Sc-0.2Si-0.1Fe	90	598	B_c	16	—	~1[e]	723	5.6×10^{-2}	2000	Musin *et al.* (2004) [61]
Al-4.5Mg-0.22Sc-0.15Zr	90	473	B_c	6	—	~0.5	723	1.0×10^{0}	880	Perevezentsev *et al.* (2004) [62]
Al-1Mg-0.2Sc	90	RT	B_{cz}[f]	4	—	~0.5	673	1.0×10^{-3}	440	Kamachi *et al.* (2004) [63]
Al-3.2Mg-0.13Sc	90	473	B_c	4	Cold-rolling	~0.2 – 0.4[c]	723	5.0×10^{-3}	810	Park *et al.* (2004) [64]
Al-3Mg-0.2Sc	90	RT	B_c	8	—	~0.2	673	3.3×10^{-2}	580	Sakai *et al.* (2004) [65] (2005) [66][g]
Al-4.1Mg-2Li-0.16Sc-0.08Zr (Al1421)	90	673	B_{cz}[f]	16	—	~2.6	723	1.4×10^{-2}	3000	Kaibyshev *et al.* (2005) [67]
Al-1.5Mg-0.2Sc-0.18Zr	90	423	B_c	6	—	~1.4 – 1.6[h]	710	1.0×10^{-2}	>900[i]	Málek *et al.* (2007) [68]
Al-4.5Mg-0.2Sc-0.2Zr	90	523	B_c	6	—	~0.3 – 1.0	773	4.5×10^{-2}	2130	Turba *et al.* (2007) [69]
Al-5Mg-0.18Mn-0.2Sc-0.08Zr (Al1570c)	90	598	B_{cz}[f]	10	—	~1	723	5.6×10^{-2}	4100	Avtokratova *et al.* (2012) [70]
Al-5Mg-0.18Mn-0.2Sc-0.08Zr (Al1570c)	90	598	B_{cz}[f]	8	—	~1	748	5.6×10^{-2}	3300	Avtokratova *et al.* (2012) [71]
Al-5.4Mg-0.2Sc-0.07Zr (Al1570c)	90	573	B_{cz}[f]	12	—	~0.6	723	1.4×10^{-1}	2400	Kaibyshev *et al.* (2013) [72]
Al-5.8Mg-0.4Mn-0.32Sc-0.1Zr (Al1570c)	90	598	B_{cz}[f]	8	Warm-rolling at 598 K	~1	723	1.4×10^{-1}	2330	Avtokratova *et al.* (2015) [73]

Table 2 continued

Alloy or composition (wt.%)	ECAP processing				Metal-working procedure after ECAP	Grain size (μm)	Superplasticity			Reference
	Channel angle (°)	Processing temperature (K)	Processing route	Nº of passes			Testing temperature (K)	Strain rate (s^{-1})	Maximum elongation (%)	
Al-6Mg-0.5Mn-0.2Sc-0.07Zr (Al1570)	90	573	B_{cz}[f]	12	Warm-rolling at 573 K	~0.3 – 0.6	723	1.4×10^{-1}	1970	Dubyna *et al.* (2016) [74]
Al-4.6Mg-0.35Mn-0.2Sc-0.09Zr (Al5024)	90	573	B_{cz}[f]	12	Cold-rolling	~0.3 – 1.8	723	1.4×10^{-1}	1440	Mogucheva *et al.* (2016) [75]
Al-4.6Mg-0.35Mn-0.2Sc-0.09Zr (Al5024)	90	573	B_{cz}[f]	12	—	~0.7	548	5.6×10^{-3}	1200	Yuzbekova *et al.* (2016) [76]
Al-4.6Mg-0.35Mn-0.2Sc-0.09Zr (Al5024)	90	573	B_{cz}[f]	12	—	~0.7	723	5.6×10^{-1}	3300	Yuzbekova *et al.* (2016) [77]
Al-3Mg-0.2Sc	90	RT	B_c	8	—	~1.8[j]	673	3.3×10^{-3}	980	Pereira *et al.*(2017)[g] [78]
Al-3Mg-0.2Sc	90	RT	B_c	8	—	~1.1[j]	523	1.0×10^{-3}	540	Pereira *et al.*(2017)[g] [79]
Al-3Mg-0.2Sc	90	600	B_c	10	—	~1.4[j]	523	1.0×10^{-3}	560	Pereira *et al.*(2017)[g] [79]

[a] First report of superplasticity in Al-Mg-Sc alloys after SPD.
[b] Elongation after solution treatment at 873 K and further ECAP processing. At higher solution treatment temperatures, more particles are precipitated and the tensile elongations are superior.
[c] Grain size measured after ECAP.
[d] The number of passes in which the maximum elongation was attained was not specified. Nevertheless, it was reported that ECAP processing was conducted for the total of 6 to 8 passes.
[e] Grain size measured after annealing at 443 K for 4 h.
[f] ECAP was conducted using plate samples.
[g] Tensile testing conducted in miniature tensile specimens.
[h] Grain size measured after annealing at 710 K for 1 h.
[i] Maximum possible elongation detected by the tensile testing facility used in the referred study.
[j] Grain size in the gauge area after tensile testing.

Table 3

Reports of superplasticity in Al-Mg-Sc alloys after HPT.

Alloy or composition (wt.%)	HPT processing				Grain size (μm)	Superplasticity				Reference
	Geometry of the HPT sample (mm)[a]	Pressure (GPa)	Processing temperature (K)	Nº of turns		Testing temperature (K)	Strain rate (s^{-1})	Maximum elongation (%)	Sample size (mm)[b]	
Al-3Mg-0.2Sc	Disc (10 × 0.8)	6	RT	5	~0.15	673	3.3×10^{-2}	500	1 × 1 × 0.6	Sakai *et al.* (2005) [66]
Al-5.6Mg-0.4Mn-0.32Sc (Al1570)	Disc (20 × 1.5)	6	RT	5	~0.12	673	1.0×10^{-2}	1460	2.8	Perevezentsev *et al.* (2007) [80]
Al-3Mg-0.2Sc	Bulk sample (10 × 8.57)	1	RT	2	~0.13	573	3.3×10^{-3}	1600	1 × 1 × 1	Horita and Langdon (2008) [81]
Al-3Mg-0.2Sc	Ring sample (40 × 3 × 0.8)	1.25	RT	1	~0.22	573	3.3×10^{-3}	1510	1 × 1 × 0.6	Harai *et al.* (2009) [82]
Al-3Mg-0.2Sc	Disc (10 × 0.8)	6	RT	10	~0.14	523	4.5×10^{-3}	850	1.1× 1 × 0.6	Pereira *et al.* (2015) [83]
Al-3Mg-0.2Sc	Disc (10 × 0.8)	6	RT	10	~1.1[c]	523	1.0×10^{-3}	620	1.1× 1 × 0.6	Pereira *et al.*(2017) [79]
Al-3Mg-0.2Sc	Disc (10 × 0.8)	6	450	10	~1.0[c]	523	1.0×10^{-3}	1020	1.1× 1 × 0.6	Pereira *et al.*(2017) [79]

[a] Diameter × thickness for the discs, diameter × height for the bulk samples and outer diameter × width × thickness for the rings.
[b] Gauge length or gauge length × gauge width × thickness of the tensile specimens.
[c] Grain size in the gauge area after tensile testing.

Table 4

Reports of superplasticity in Al-Mg-Sc alloys after friction stir processing.

Alloy or composition (wt.%)	Friction stir processing - FSP			Grain size (μm)	Superplasticity				Reference
	Geometry of the FSP tool (mm)[a]	Rotation rate of the FSP tool (rpm)	Traverse speed (mm min^{-1})		Testing temperature (K)	Strain rate (s^{-1})	Maximum elongation (%)	Sample size (mm)[b]	
Al-8.9Zn-2.6Mg-0.09Sc	11.4 × 4.2 × 3.2	400	25.4	~0.68	583	3.0×10^{-2}	1165	1.3 × 1 × 0.5	Charit and Mishra (2005) [84]
Al-5.3Mg-0.5Mn-0.23Sc-0.14Fe-0.06Zr	14 × 3.5 × 4.5	600	25	~2.6	723	1.0×10^{-1}	2150	2.5 × 1.4 × 0.8	Liu and Ma (2008) [85]
Al-5.3Mg-0.49Mn-0.23Sc-0.14Fe-0.06Zr	14 × 3.5 × 4.5	400	100	~0.7	573	3.0×10^{-2}	620	2.5 × 1.4 × 0.8	Liu *et al.* (2009) [86]
Al-5.3Mg-0.49Mn-0.23Sc-0.14Fe-0.06Zr	14 × 3.5 × 4.5	400	25	~0.6	573	1.0×10^{-2}	560	2.5 × 1.4 × 0.8	Liu and Ma (2010) [87]
Al-5.3Mg-0.49Mn-0.23Sc-0.14Fe-0.06Zr	14 × 3.5 × 4.5	400	25	~2.2	748	1.0×10^{-1}	1500	2.5 × 1.4 × 0.8	Liu *et al.* (2012) [88]
Al-4.7Mg-0.35Sc-0.17Zr	16 × 2.4 × 3.9	95	73	~1.3	773	5.0×10^{-2}	>1900[c]	10 × 5.4 × 2	Smolej *et al.* (2014) [89]
Al-5.16Mg-0.18Sc-0.15Zr	16 × 2.4 × 3.9	95	73	~1.7	773	1.0×10^{-1}	>1900[c]	10 × 5.4 × 2	Smolej *et al.* (2014) [90]

[a] Concave shoulder diameter × threaded pin diameter × threaded pin length.
[b] Gauge length × gauge width × thickness of the tensile specimens.
[c] Maximum possible elongation detected by the tensile testing facility used in the referred study.